

EUROPEAN ORGANIZATION FOR NUCLEAR RESEARCH (CERN)



CERN-PH-EP-2015-076

LHCb-PAPER-2015-004

March 24, 2015

Measurement of CP violation in $B^0 \rightarrow J/\psi K_s^0$ decays

The LHCb collaboration[†]

Abstract

Measurements are presented of the CP violation observables S and C in the decays of B^0 and \bar{B}^0 mesons to the $J/\psi K_s^0$ final state. The data sample corresponds to an integrated luminosity of 3.0 fb^{-1} collected with the LHCb experiment in proton-proton collisions at center-of-mass energies of 7 and 8 TeV. The analysis of the time evolution of 41 500 B^0 and \bar{B}^0 decays yields $S = 0.731 \pm 0.035 \text{ (stat)} \pm 0.020 \text{ (syst)}$ and $C = -0.038 \pm 0.032 \text{ (stat)} \pm 0.005 \text{ (syst)}$. In the Standard Model, S equals $\sin(2\beta)$ to a good level of precision. The values are consistent with the current world averages and with the Standard Model expectations.

Submitted to Phys. Rev. Lett.

© CERN on behalf of the LHCb collaboration, license CC-BY-4.0.

[†]Authors are listed at the end of this Letter.

The violation of charge-parity (CP) conservation in processes involving B mesons was first observed in the “golden mode” $B^0 \rightarrow J/\psi K_s^0$ by the BaBar and Belle experiments at the asymmetric e^+e^- colliders PEP-II and KEKB [1, 2]. Since then, measurements of CP violation in this decay mode have reached a precision at the level of 10^{-2} [3, 4]. Thus, these measurements play an important role in constraining and testing the quark-flavor sector of the Standard Model [5, 6], which relates CP -violating observables to a single irreducible phase in the Cabibbo-Kobayashi-Maskawa (CKM) quark-mixing matrix [7, 8]. As the $J/\psi K_s^0$ final state is common to both the B^0 and the \bar{B}^0 meson decays, the interference between the amplitudes for the direct decay and for the decay after $B^0-\bar{B}^0$ oscillation results in a decay-time dependent CP asymmetry between the time-dependent decay rates of B^0 and \bar{B}^0 mesons,

$$\mathcal{A}(t) \equiv \frac{\Gamma(\bar{B}^0(t) \rightarrow J/\psi K_s^0) - \Gamma(B^0(t) \rightarrow J/\psi K_s^0)}{\Gamma(\bar{B}^0(t) \rightarrow J/\psi K_s^0) + \Gamma(B^0(t) \rightarrow J/\psi K_s^0)} = \frac{S \sin(\Delta m t) - C \cos(\Delta m t)}{\cosh(\frac{\Delta \Gamma t}{2}) + A_{\Delta \Gamma} \sinh(\frac{\Delta \Gamma t}{2})}. \quad (1)$$

Here, $B^0(t)$ and $\bar{B}^0(t)$ indicate the flavor of the B meson at production, while t indicates the decay time. The parameters Δm and $\Delta \Gamma$ are the mass and the decay width differences between the heavy and light mass eigenstates of the $B^0-\bar{B}^0$ system, and S , C , and $A_{\Delta \Gamma}$ are CP observables. As $\Delta \Gamma$ is negligible for the $B^0-\bar{B}^0$ system [9], the time-dependent asymmetry simplifies to $\mathcal{A}(t) = S \sin(\Delta m t) - C \cos(\Delta m t)$.

The $B^0 \rightarrow J/\psi K_s^0$ decay is dominated by a $\bar{b} \rightarrow c\bar{c}\bar{s}$ transition,¹ and CP violation in the decay is expected to be negligible at the current level of experimental precision, giving $C \approx 0$. This allows to identify S with $\sin(2\beta)$, where $\beta \equiv \arg[-(V_{cd}V_{cb}^*)/(V_{td}V_{tb}^*)]$ is one of the angles of the CKM triangle. Other measurements that constrain this triangle predict $\sin(2\beta)$ as 0.771 ± 0.017 [10], giving a small discrepancy with respect to the average of direct measurements, 0.682 ± 0.019 [9], where the most precise input comes from a CP violation measurement in $B^0 \rightarrow J/\psi K_s^0$ decays by the Belle experiment, $S = 0.670 \pm 0.029$ (stat) ± 0.013 (syst) [4]. To clarify the CKM picture, both better experimental precision and improved understanding of higher-order contributions to the decay amplitudes are required [11, 12].

The analysis presented in this Letter supersedes a previous measurement by LHCb [13], which was performed on data corresponding to an integrated luminosity of 1.0 fb^{-1} at a center-of-mass energy of 7 TeV . By adding data corresponding to 2 fb^{-1} at 8 TeV and using an optimized selection and additional “flavor tagging” algorithms to identify the quark content of the B meson at production, we increase the statistical power of the analysis by almost a factor 6.

The LHCb detector [14, 15] is a single-arm forward spectrometer covering the pseudorapidity range $2 < \eta < 5$, designed for the study of particles containing b or c quarks. The detector includes a high-precision tracking system consisting of a silicon-strip vertex detector surrounding the pp interaction region, a large-area silicon-strip detector located upstream of a dipole magnet, and three stations of silicon-strip detectors and straw drift

¹Mention of a particular decay mode implies the inclusion of charge-conjugate states except when the measurement of CP violation is involved.

tubes placed downstream of the magnet. Different types of charged hadrons are distinguished using information from two ring-imaging Cherenkov detectors. Photon, electron, and hadron candidates are identified by a calorimeter system consisting of scintillating-pad and preshower detectors, an electromagnetic calorimeter, and a hadronic calorimeter. Muons are identified by a system composed of alternating layers of iron and multiwire proportional chambers. The online event selection system (trigger) [16] consists of a hardware stage, based on information from the calorimeter and muon systems, followed by a software stage.

The analysis is performed with $B^0 \rightarrow J/\psi K_s^0$ candidates reconstructed in the $J/\psi \rightarrow \mu^+ \mu^-$ and $K_s^0 \rightarrow \pi^+ \pi^-$ final states. Two oppositely charged particles, identified as muons with high momentum and high transverse momentum, are required to originate from a common space-point (vertex) and to have an invariant mass in a range $\pm 60 \text{ MeV}/c^2$ around the known J/ψ mass [17]. Since the B^0 meson has a lifetime of 1.5 ps and has high momentum, the resulting J/ψ candidate is required to be significantly separated from all reconstructed pp collision points (primary vertices (PVs)). The K_s^0 candidates are formed from two oppositely charged, high-momentum pion candidates with a clear separation from any PV in the event. Candidates decaying early enough for the final-state pions to be reconstructed in the vertex detector are characterized as *long* candidates and are required to have an invariant mass within $\pm 15 \text{ MeV}/c^2$ of the known K_s^0 mass [17]. The K_s^0 candidates that decay later, such that track segments of the pions cannot be formed in the vertex detector, are called *downstream* candidates; these have a larger momentum resolution than the long candidates, and thus the corresponding $\pi^+ \pi^-$ pairs are required to have an invariant mass within $\pm 55 \text{ MeV}/c^2$ of the known K_s^0 mass. A good vertex fit quality and sufficient separation from the B^0 decay vertex are required for the K_s^0 candidate's decay vertex. To eliminate background contributions from $\Lambda_b^0 \rightarrow J/\psi \Lambda$ decays, the π^+ (π^-) candidate has to fulfill particle identification requirements if the invariant mass under a $p\pi^-$ ($\pi^+\bar{p}$) mass hypothesis is compatible with the Λ mass.

The B^0 candidates are reconstructed from J/ψ and K_s^0 candidates that form a good quality vertex. Their decay time t is obtained from a fit to the full decay chain while constraining the production vertex of the B^0 to the associated PV [18]. The reconstructed B^0 candidate mass m is obtained from a similar fit with the $\mu^+ \mu^-$ and $\pi^+ \pi^-$ invariant masses constrained to the known J/ψ and K_s^0 masses. The latter fit must satisfy loose requirements on its quality, and resulting candidates are only retained if $5230 < m < 5330 \text{ MeV}/c^2$ and $0.3 < t < 18.3 \text{ ps}$. The fit uncertainty σ_t on the decay time is required to be smaller than 200 fs, which is well above the average resolution of 55 fs (65 fs) for candidates with long (downstream) K_s^0 daughters. The quantity σ_t is used later in the analysis as an estimate of the per-candidate decay-time resolution. Multiple PVs and, in a small fraction of events, multiple $B^0 \rightarrow J/\psi K_s^0$ candidates, lead to multiple (B^0 , PV) pairs per event. In such cases, one pair is chosen at random.

Various simulated data samples are used in the analysis. In the simulation, pp collisions are generated using PYTHIA [19] with a specific LHCb configuration [20]. Decays of hadronic particles are described by EvtGen [21]. The interaction of the generated particles with

the detector, and its response, are implemented using the GEANT4 toolkit [22] as described in Ref. [23].

Tagging algorithms are used to infer the initial flavor of the B meson candidate, *i.e.* whether it contained a b or a \bar{b} quark at production. Each algorithm provides a decision d on the flavor of the B meson candidate (tag), and an estimate η of the probability for that decision to be incorrect (mistag probability). The knowledge of the B meson production flavor is essential for this analysis, and so only candidates for which the tagging algorithms yield a decision are considered.

One class of flavor tagging algorithms, the opposite-side tagger (OS), exploits the dominant production mechanism of b hadrons, *i.e.* the production of $b\bar{b}$ quark pairs, by reconstructing the b hadron produced in association with the signal B meson. The OS tagger uses the charge of the electron or muon from semileptonic b decays, the charge of the kaon from the $b \rightarrow c \rightarrow s$ decay chain, and the inclusive charge of particles associated with the secondary vertex reconstructed from the b hadron decay products; further details are described in Ref. [24].

A major improvement in this analysis over Ref. [13] is the inclusion of the same-side pion tagger (SS π), which deduces the production flavor by exploiting pions produced in the fragmentation of the b quark that produced the signal B meson or in the decay of excited B mesons into the signal B meson [25, 26]. Tagging pion candidates are selected requiring charged, high momentum and high transverse-momentum particles that are consistent with originating from the associated PV. Pions are identified using information from the particle identification detectors, and the difference between the invariant mass of the B and the $B\pi^\pm$ pair is required to be less than $1.2\text{ GeV}/c^2$. Additionally, the flight directions of the pion and the B candidate must be compatible. If multiple pion candidates pass the selection, the one with the highest transverse momentum is used. The mistag probability is obtained using a neural network which is trained on simulated events and whose inputs are global event properties and kinematic and geometric information on the pion and B signal candidates.

The tagging calibration is performed in control samples of B mesons whose final state determines the B flavor at decay time, by determining a linear correction $\omega(\eta)$ that relates the estimated mistag probability η with the mistag probability ω observed in the control sample. To account for asymmetries in the detection efficiency of charged particles, which can lead to different mistag probabilities for B^0 and \bar{B}^0 mesons, an additional linear correction function $\Delta\omega(\eta)$ is determined. Asymmetries in the efficiency of the algorithms in determining a decision are found to be negligible.

The $B^+ \rightarrow J/\psi K^+$ decay is used to determine the flavor tagging calibration for the OS tagger. A consistency check of the calibration is performed in a control sample of $B^0 \rightarrow J/\psi K^{*0}$ decays, showing a good correspondence of the calibration between B^+ and B^0 decays. As the quarks that accompany the b quark in B^+ and B^0 mesons differ, the SS π tagger calibration is performed with $B^0 \rightarrow J/\psi K^{*0}$ decays [27]. Systematic uncertainties are assigned for the uncertainties associated with the calibration method and for the validity of the calibration in the signal decay mode. A summary of the calibration results is given in the Appendix.

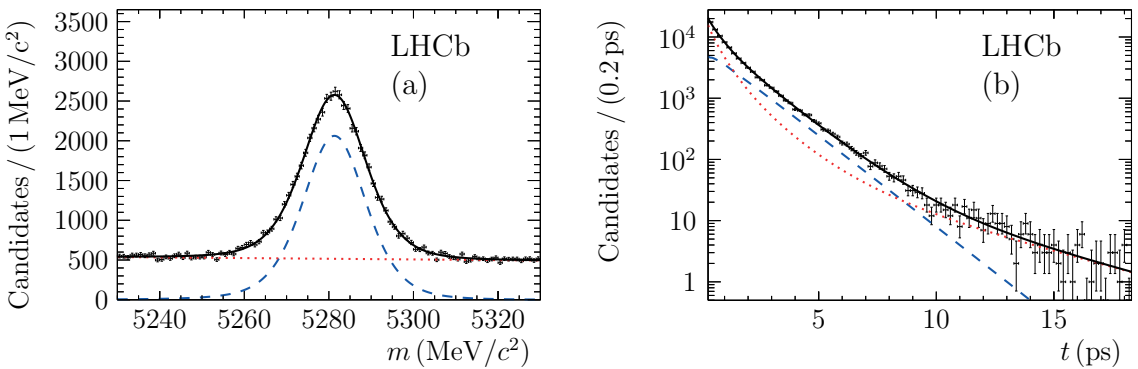


Figure 1: Distribution of (a) the reconstructed mass and (b) logarithmic distribution of the decay time of tagged $B^0 \rightarrow J/\psi K_s^0$ candidates. The solid black lines show the fit projections, while the dashed (dotted) lines show the projections for the signal (background) components only.

The effective tagging efficiency is the product of the probability for reaching a tagging decision, $\varepsilon_{\text{tag}} = (36.54 \pm 0.14)\%$, and the square of the effective dilution, $D \equiv 1 - 2\omega = (28.75 \pm 0.24)\%$, which corresponds to an effective mistag probability of $\omega = (35.62 \pm 0.12)\%$. Compared to the previous LHCb analysis [13] the effective tagging efficiency $\varepsilon_{\text{eff}} = \varepsilon_{\text{tag}} D^2$ increases from 2.38% to 3.02%, mainly due to the inclusion of the SS π tagger.

The values of the CP violation observables S and C are estimated by maximizing the likelihood of a probability density function (PDF) describing the unbinned distributions of the following observables: the reconstructed mass m , the decay time t and its uncertainty estimate σ_t , the OS and SS π flavor tag decisions d_{OS} and $d_{\text{SS}\pi}$, and the corresponding per-candidate mistag probability estimates η_{OS} and $\eta_{\text{SS}\pi}$. The fit is performed simultaneously in 24 independent subsamples, chosen according to data-taking conditions (7 TeV, 8 TeV), K_s^0 type (downstream, long), flavor tagging algorithm (OS only, SS π only, OS and SS π), and two trigger requirements. In each category the data distribution is modeled using a sum of two individual PDFs, one for the B^0 signal and one for the combinatorial background.

The reconstructed mass of the signal component is parametrized with a double-sided Hypatia PDF [28] with tail parameters determined from simulation. An exponential function is used to model the background component, with independent parameters for the downstream and long K_s^0 subsamples. The fit to the mass distributions yields $41\,560 \pm 270$ tagged $B^0 \rightarrow J/\psi K_s^0$ signal decays. The mass distribution and projections of the PDFs are shown in Fig. 1 (a).

The decay-time resolution is modeled by a sum of three Gaussian functions with common mean, but different widths, which are convolved with the PDFs describing the decay-time distributions. Two of the widths are given by the per-candidate resolution estimate σ_t , each calibrated with independent linear calibration functions. The third Gaussian describes the resolution for candidates associated to a wrong PV. The scale and width parameters are obtained in a fit to the decay-time distribution of a control sample of

B^0 candidates formed from prompt J/ψ and K_s^0 mesons. The parameters are determined separately for candidates formed from downstream and long K_s^0 candidates.

Trigger, reconstruction, and selection criteria distort the measured B^0 decay-time distribution, leading to a decay-time dependent efficiency. Effects of the trigger requirements, which distort the decay-time distribution at low decay times, are determined using data. The misreconstruction of tracks leads to inefficiencies at large decay times. To account for this effect, an additional decay-time dependent efficiency of the form $e^{-\beta_t t}$ is used, where β_t is obtained from simulation.

The PDF of true decay times t' is given by

$$\begin{aligned} & \mathcal{P}(t', d_{\text{OS}}, d_{\text{SS}\pi} | \eta_{\text{OS}}, \eta_{\text{SS}\pi}) \\ &= \sum_{d'} \left[\prod_j \zeta(d_j, \eta_j, d') \right] (1 - d' A_{\text{P}}) e^{-t'/\tau} \{1 - d' S \sin(\Delta m t') + d' C \cos(\Delta m t')\}, \end{aligned} \quad (2)$$

where the tag decision d takes the value $+1$ (-1) for a tagged B^0 (\bar{B}^0) candidate and d' takes the value $+1$ (-1) for the B^0 (\bar{B}^0) component of the signal distribution, τ is the B^0 meson lifetime, and

$$\zeta(d_j, \eta_j, d') = 1 + d_j \left(1 - 2 \left[\omega(\eta_j) + d' \frac{\Delta\omega(\eta_j)}{2} \right] \right) \quad (3)$$

represents the calibration of the tagging response from the tagging algorithm $j = \{\text{OS, SS}\pi\}$. The production asymmetry $A_{\text{P}} \equiv [\sigma(\bar{B}^0) - \sigma(B^0)]/[\sigma(\bar{B}^0) + \sigma(B^0)]$, where σ denotes the production cross-section inside the LHCb acceptance, is obtained using a measurement in 7 TeV pp collisions [29]. Considering differences between the 7 and 8 TeV data-taking conditions, the production asymmetries are determined as $A_{\text{P}}^{7\text{TeV}} = -0.0108 \pm 0.0052$ (stat) ± 0.0014 (syst) and $A_{\text{P}}^{8\text{TeV}} = A_{\text{P}}^{7\text{TeV}} + \Delta A_{\text{P}}$ with $\Delta A_{\text{P}} = 0.0004 \pm 0.0018$ (syst) [30]. The background decay-time distribution is parametrized by a sum of exponential functions, convolved with the resolution model used for the signal. This parametrization does not depend on the tag decision and mistag probability estimates. The number of required exponential functions varies across subsamples. The decay-time distribution and projections of the PDFs are shown in Fig. 1(b). The distributions of the per-candidate resolution estimate σ_t and the per-candidate mistag probabilities, η_{OS} and $\eta_{\text{SS}\pi}$, are modeled by empirical functions. Independent parameterizations are chosen for the signal and background components.

The likelihood is a function of 83 free parameters, including S and C , and 48 yield parameters for the signal and the background components in 24 individual subsamples. Eleven parameters are external inputs, including the production asymmetry, the flavor tagging calibration parameters, and the mass difference Δm [17]. These are constrained in the fit within their statistical uncertainties and taking their correlations into account. The likelihood fit yields $S = 0.729 \pm 0.035$ and $C = -0.033 \pm 0.032$ with a correlation coefficient of $\rho(S, C) = 0.483$. Fig. 2 shows the decay-time dependent signal-yield asymmetry. An additional fit with fixed $C = 0$ yields $S = 0.746 \pm 0.030$. Corrections of $+0.002$ for S

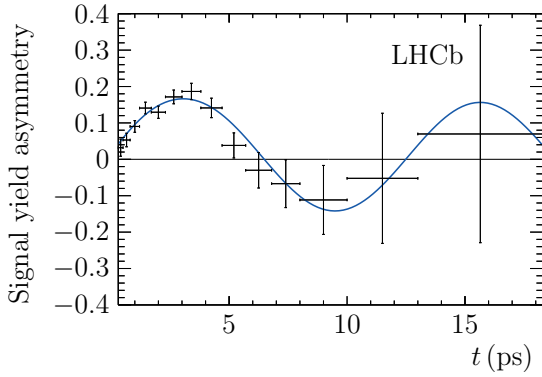


Figure 2: Time-dependent signal-yield asymmetry $(N_{\bar{B}^0} - N_{B^0})/(N_{\bar{B}^0} + N_{B^0})$. Here, N_{B^0} ($N_{\bar{B}^0}$) is the number of $B^0 \rightarrow J/\psi K_s^0$ decays with a B^0 (\bar{B}^0) flavor tag. The data points are obtained with the *sPlot* technique [32], assigning signal weights to the events based on a fit to the reconstructed mass distribution. The solid curve is the projection of the signal PDF.

and -0.005 for C are applied to account for CP violation in $K^0-\bar{K}^0$ mixing and for the difference in the nuclear cross-sections in material between K^0 and \bar{K}^0 states [31]. The correction is negligible for the result for S with $C = 0$.

Various sources of systematic uncertainties on the CP observables are examined, in particular from mismodeling PDFs and from systematic uncertainties on the input parameters. In each study, a large set of pseudoexperiments is simulated using a PDF modified such as to include the systematic effect of interest; the relevant distributions from these pseudoexperiments are then fitted with the nominal PDF. Significant average deviations of the fit results from the input values are used as estimates of systematic uncertainties. The largest systematic uncertainty on S , ± 0.018 , accounts for possible tag asymmetries in the background; for C the largest uncertainty, ± 0.0034 , results from the systematic uncertainty on Δm . Systematic uncertainties on the flavor tagging calibration account for the second largest systematic uncertainty on S , ± 0.006 , and on C , ± 0.0024 . The third largest uncertainty on S , ± 0.005 , arises from assuming $\Delta\Gamma = 0$ and is evaluated by generating pseudoexperiments with $\Delta\Gamma$ set to the value of its current uncertainty, 0.007 ps^{-1} [9], and then neglecting it in the fit. Remaining uncertainties due to neglecting correlations between the reconstructed mass and decay time of the candidates, mismodeling of the decay-time resolution and efficiency, the systematic uncertainty of the production asymmetry, and the uncertainty on the length scale of the vertex detector are small and are given in the Appendix. Adding all contributions in quadrature results in total systematic uncertainties of ± 0.020 on S and ± 0.005 on C .

Several consistency checks are performed by splitting the data set according to different data-taking conditions, tagging algorithms, and different reconstruction and trigger requirements. All results show good agreement with the nominal results.

In conclusion, a measurement of CP violation in the interference between the direct decay and the decay after $B^0-\bar{B}^0$ oscillation to a $J/\psi K_s^0$ final state is performed using 41 500 flavor-tagged $B^0 \rightarrow J/\psi K_s^0$ decays reconstructed with the LHCb detector in a

sample of proton-proton collisions at center-of-mass energies of 7 and 8 TeV, corresponding to an integrated luminosity of 3.0 fb^{-1} . The CP observables S and C , which allow the determination of the CKM angle β , are measured to be

$$S = 0.731 \pm 0.035 \text{ (stat)} \pm 0.020 \text{ (syst)}, \\ C = -0.038 \pm 0.032 \text{ (stat)} \pm 0.005 \text{ (syst)},$$

with a statistical correlation coefficient $\rho(S, C) = 0.483$. When C is fixed to zero the measurement yields $S = \sin(2\beta) = 0.746 \pm 0.030$ (stat). This measurement supersedes the previous LHCb result obtained with 1.0 fb^{-1} [13], and represents the most precise time-dependent CP violation measurement at a hadron collider to date. Furthermore, the result has a similar precision to, and is in good agreement with, previous measurements performed at the Belle and BaBar experiments at the KEKB and PEP-II colliders [3, 4]. This result is in excellent agreement with the expectations from other measurements and improves the consistency of the CKM sector of the Standard Model.

Acknowledgements

We express our gratitude to our colleagues in the CERN accelerator departments for the excellent performance of the LHC. We thank the technical and administrative staff at the LHCb institutes. We acknowledge support from CERN and from the national agencies: CAPES, CNPq, FAPERJ and FINEP (Brazil); NSFC (China); CNRS/IN2P3 (France); BMBF, DFG, HGF and MPG (Germany); INFN (Italy); FOM and NWO (The Netherlands); MNiSW and NCN (Poland); MEN/IFA (Romania); MinES and FANO (Russia); MinECo (Spain); SNSF and SER (Switzerland); NASU (Ukraine); STFC (United Kingdom); NSF (USA). The Tier1 computing centres are supported by IN2P3 (France), KIT and BMBF (Germany), INFN (Italy), NWO and SURF (The Netherlands), PIC (Spain), GridPP (United Kingdom). We are indebted to the communities behind the multiple open source software packages on which we depend. We are also thankful for the computing resources and the access to software R&D tools provided by Yandex LLC (Russia). Individual groups or members have received support from EPLANET, Marie Skłodowska-Curie Actions and ERC (European Union), Conseil général de Haute-Savoie, Labex ENIGMASS and OCEVU, Région Auvergne (France), RFBR (Russia), XuntaGal and GENCAT (Spain), Royal Society and Royal Commission for the Exhibition of 1851 (United Kingdom).

References

- [1] BaBar collaboration, B. Aubert *et al.*, *Observation of CP violation in the B^0 meson system*, Phys. Rev. Lett. **87** (2001) 091801, [arXiv:hep-ex/0107013](https://arxiv.org/abs/hep-ex/0107013).
- [2] Belle collaboration, K. Abe *et al.*, *Observation of large CP violation in the neutral B meson system*, Phys. Rev. Lett. **87** (2001) 091802, [arXiv:hep-ex/0107061](https://arxiv.org/abs/hep-ex/0107061).

- [3] BaBar collaboration, B. Aubert *et al.*, *Measurement of time-dependent CP asymmetry in $B^0 \rightarrow c\bar{c}K^{(*)0}$ decays*, Phys. Rev. **D79** (2009) 072009, [arXiv:0902.1708](https://arxiv.org/abs/0902.1708).
- [4] Belle collaboration, I. Adachi *et al.*, *Precise measurement of the CP violation parameter $\sin 2\phi_1$ in $B^0 \rightarrow (c\bar{c})K^0$ decays*, Phys. Rev. Lett. **108** (2012) 171802, [arXiv:1201.4643](https://arxiv.org/abs/1201.4643).
- [5] A. B. Carter and A. I. Sanda, *CP violation in B meson decays*, Phys. Rev. **D23** (1981) 1567.
- [6] I. I. Y. Bigi and A. I. Sanda, *Notes on the observability of CP violations in B decays*, Nucl. Phys. **B193** (1981) 85.
- [7] N. Cabibbo, *Unitary symmetry and leptonic decays*, Phys. Rev. Lett. **10** (1963) 531.
- [8] M. Kobayashi and T. Maskawa, *CP violation in the renormalizable theory of weak interaction*, Prog. Theor. Phys. **49** (1973), no. 2 652.
- [9] Heavy Flavor Averaging Group (HFAG), Y. Amhis *et al.*, *Averages of b-hadron, c-hadron, and τ -lepton properties as of summer 2014*, [arXiv:1412.7515](https://arxiv.org/abs/1412.7515), updated results and plots available at: <http://www.slac.stanford.edu/xorg/hfag/>.
- [10] J. Charles *et al.*, *Current status of the Standard Model CKM fit and constraints on $\Delta F = 2$ New Physics*, [arXiv:1501.05013](https://arxiv.org/abs/1501.05013).
- [11] LHCb collaboration, R. Aaij *et al.*, *Measurement of the time-dependent CP asymmetries in $B_s^0 \rightarrow J/\psi K_s^0$* , [arXiv:1503.07055](https://arxiv.org/abs/1503.07055), submitted to JHEP; LHCb collaboration, R. Aaij *et al.*, *Measurement of the CP-violating phase β in $B^0 \rightarrow J/\psi \pi^+ \pi^-$ decays and limits on penguin effects*, Phys. Lett. **B742** (2015) 38, [arXiv:1411.1634](https://arxiv.org/abs/1411.1634).
- [12] K. De Bruyn and R. Fleischer, *A roadmap to control penguin effects in $B_d^0 \rightarrow J/\psi K_s^0$ and $B_s^0 \rightarrow J/\psi \phi$* , [arXiv:1412.6834](https://arxiv.org/abs/1412.6834); P. Frings, U. Nierste, and M. Wiebusch, *Penguin contributions to CP phases in $B_{d,s}$ decays to charmonium*, [arXiv:1503.00859](https://arxiv.org/abs/1503.00859).
- [13] LHCb collaboration, R. Aaij *et al.*, *Measurement of the time-dependent CP asymmetry in $B^0 \rightarrow J/\psi K_s^0$ decays*, Phys. Lett. **B721** (2013) 24, [arXiv:1211.6093](https://arxiv.org/abs/1211.6093).
- [14] LHCb collaboration, A. A. Alves, Jr. *et al.*, *The LHCb detector at the LHC*, JINST **3** (2008) S08005.
- [15] LHCb collaboration, R. Aaij *et al.*, *LHCb detector performance*, Int. J. Mod. Phys. **A30** (2015) 1530022, [arXiv:1412.6352](https://arxiv.org/abs/1412.6352).
- [16] R. Aaij *et al.*, *The LHCb trigger and its performance in 2011*, JINST **8** (2013) P04022, [arXiv:1211.3055](https://arxiv.org/abs/1211.3055).
- [17] Particle Data Group, K. A. Olive *et al.*, *Review of particle physics*, Chin. Phys. **C38** (2014) 090001.

- [18] W. D. Hulsbergen, *Decay chain fitting with a Kalman filter*, Nucl. Instrum. Meth. **A552** (2005) 566, [arXiv:physics/0503191](#).
- [19] T. Sjöstrand, S. Mrenna, and P. Skands, *PYTHIA 6.4 physics and manual*, JHEP **05** (2006) 026, [arXiv:hep-ph/0603175](#); T. Sjöstrand, S. Mrenna, and P. Skands, *A brief introduction to PYTHIA 8.1*, Comput. Phys. Commun. **178** (2008) 852, [arXiv:0710.3820](#).
- [20] I. Belyaev *et al.*, *Handling of the generation of primary events in Gauss, the LHCb simulation framework*, Nuclear Science Symposium Conference Record (NSS/MIC) IEEE (2010) 1155.
- [21] D. J. Lange, *The EvtGen particle decay simulation package*, Nucl. Instrum. Meth. **A462** (2001) 152.
- [22] Geant4 collaboration, J. Allison *et al.*, *Geant4 developments and applications*, IEEE Trans. Nucl. Sci. **53** (2006) 270; Geant4 collaboration, S. Agostinelli *et al.*, *Geant4: A simulation toolkit*, Nucl. Instrum. Meth. **A506** (2003) 250.
- [23] M. Clemencic *et al.*, *The LHCb simulation application, Gauss: Design, evolution and experience*, J. Phys. Conf. Ser. **331** (2011) 032023.
- [24] LHCb collaboration, R. Aaij *et al.*, *Opposite-side flavour tagging of B mesons at the LHCb experiment*, Eur. Phys. J. **C72** (2012) 2022, [arXiv:1202.4979](#).
- [25] M. Gronau, A. Nippe, and J. L. Rosner, *Method for flavor tagging in neutral B meson decays*, Phys. Rev. **D47** (1993) 1988, [arXiv:hep-ph/9211311](#).
- [26] LHCb collaboration, R. Aaij *et al.*, *Precise measurements of the properties of the $B_1(5721)^{0,+}$ and $B_2^*(5747)^{0,+}$ states and observation of $B^{+,0}\pi^{-,+}$ mass structures*, [arXiv:1502.02638](#), to appear in JHEP.
- [27] LHCb collaboration, R. Aaij *et al.*, *Measurement of the $B^0-\bar{B}^0$ oscillation frequency Δm_d with the decays $B^0 \rightarrow D^-\pi^+$ and $B^0 \rightarrow J/\psi K^{*0}$* , Phys. Lett. **B719** (2013) 318, [arXiv:1210.6750](#).
- [28] D. M. Santos and F. Dupertuis, *Mass distributions marginalized over per-event errors*, Nucl. Instrum. Meth. **A764** (2014) 150, [arXiv:1312.5000](#).
- [29] LHCb collaboration, R. Aaij *et al.*, *Measurement of the \bar{B}^0-B^0 and $\bar{B}_s^0-B_s^0$ production asymmetries in pp collisions at $\sqrt{s} = 7$ TeV*, Phys. Lett. **B739** (2014) 218, [arXiv:1408.0275](#).
- [30] LHCb collaboration, R. Aaij *et al.*, *Measurement of the semileptonic CP asymmetry in $B^0-\bar{B}^0$ mixing*, Phys. Rev. Lett. **114** (2015) 041601, [arXiv:1409.8586](#).

- [31] W. Fetscher *et al.*, *Regeneration of arbitrary coherent neutral kaon states: A new method for measuring the K^0 - \bar{K}^0 forward scattering amplitude*, Z. Phys. **C72** (1996) 543; B. R. Ko, E. Won, B. Golob, and P. Pakhlov, *Effect of nuclear interactions of neutral kaons on CP asymmetry measurements*, Phys. Rev. **D84** (2011) 111501(R), arXiv:1006.1938.
- [32] M. Pivk and F. R. Le Diberder, *sPlot: A statistical tool to unfold data distributions*, Nucl. Instrum. Meth. **A555** (2005) 356, arXiv:physics/0402083.

Appendix

Overview of tagging calibration parameters

The calibration functions of the mistag probability $\omega(\eta)$ and the mistag probability difference $\Delta\omega(\eta) = \omega^{B^0} - \omega^{\bar{B}^0}$ are chosen as

$$\omega(\eta) = p_1(\eta - \langle\eta\rangle) + p_0, \quad \Delta\omega(\eta) = \Delta p_1(\eta - \langle\eta\rangle) + \Delta p_0. \quad (\text{A1})$$

The OS calibration parameters are determined to be

$$\begin{aligned} p_0^{\text{OS}} &= 0.3815 \pm 0.0011 \text{ (stat)} \pm 0.0016 \text{ (syst)} , \\ p_1^{\text{OS}} &= 0.978 \pm 0.012 \text{ (stat)} \pm 0.009 \text{ (syst)} , \\ \Delta p_0^{\text{OS}} &= 0.0148 \pm 0.0016 \text{ (stat)} \pm 0.0008 \text{ (syst)} , \\ \Delta p_1^{\text{OS}} &= 0.070 \pm 0.018 \text{ (stat)} \pm 0.004 \text{ (syst)} , \\ \langle\eta^{\text{OS}}\rangle &= 0.3786 . \end{aligned} \quad (\text{A2})$$

Fig. A1 shows the raw mixing asymmetry and the calibration of the mistag estimates. The measured SS π calibration parameters are

$$\begin{aligned} p_0^{\text{SS}\pi} &= 0.4232 \pm 0.0029 \text{ (stat)} \pm 0.0028 \text{ (syst)} , \\ p_1^{\text{SS}\pi} &= 1.011 \pm 0.064 \text{ (stat)} \pm 0.031 \text{ (syst)} , \\ \Delta p_0^{\text{SS}\pi} &= -0.0026 \pm 0.0043 \text{ (stat)} \pm 0.0027 \text{ (syst)} , \\ \Delta p_1^{\text{SS}\pi} &= -0.171 \pm 0.096 \text{ (stat)} \pm 0.04 \text{ (syst)} , \\ \langle\eta^{\text{SS}\pi}\rangle &= 0.425 . \end{aligned} \quad (\text{A3})$$

In the dataset of 114000 $B^0 \rightarrow J/\psi K_s^0$ decays, the OS tagger algorithm yields a tagging power of $(2.63 \pm 0.04)\%$ and the SS π tagger algorithm yields $(0.376 \pm 0.024)\%$. For events that have both OS and SS π tagging decisions, the effective tagging power is $(0.503 \pm 0.010)\%$. The combined effective tagging power of these three overlapping tagging categories is $(3.02 \pm 0.05)\%$.

Summary of systematic uncertainties

The systematic uncertainties are summarised in Table A1. The overall systematic uncertainty is calculated by summing the single uncertainties in quadrature. The relative systematic uncertainties compared to the central values of S and C are given in brackets. Here, we set $S = 0.729$ and $C = -0.033$ as reference.

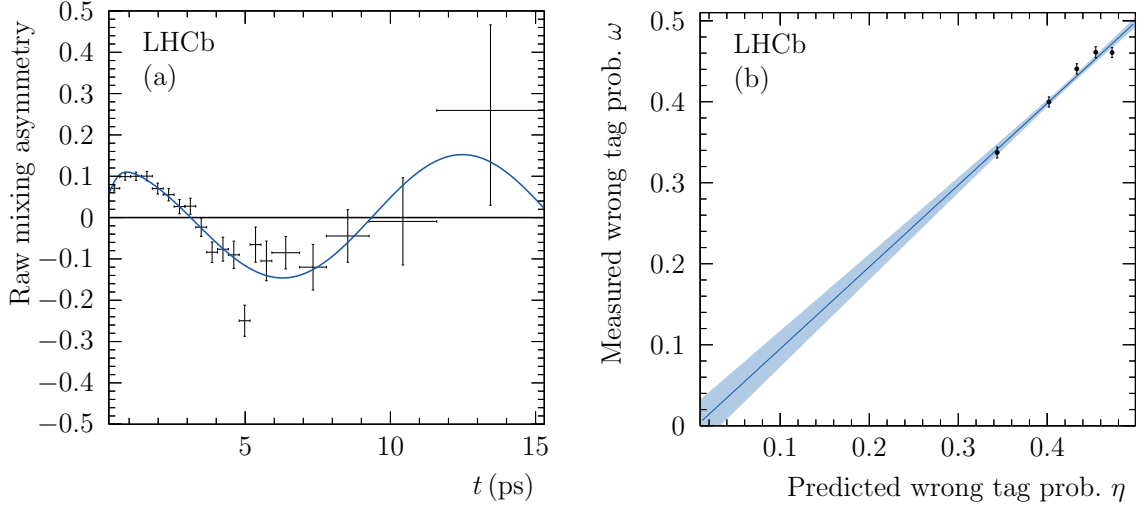


Figure A1: (a) Raw mixing asymmetry ($N_{\text{unmixed}} - N_{\text{mixed}})/(N_{\text{unmixed}} + N_{\text{mixed}})$) for all SS π tagged $B^0 \rightarrow J/\psi K^{*0}$ decay candidates. Here, N_{unmixed} (N_{mixed}) is the number of $B^0 \rightarrow J/\psi K^{*0}$ decays with a final state that does (not) correspond to the flavor tag. The black line shows the fit projection. (b) The linear calibration of the SS π mistag probability with $B^0 \rightarrow J/\psi K^{*0}$ decays.

Table A1: Systematic uncertainties σ_S and σ_C on S and C . Entries marked with a dash represent studies where no significant effect is observed.

Origin	σ_S	σ_C
Background tagging asymmetry	0.0179 (2.5%)	0.0015 (4.5%)
Tagging calibration	0.0062 (0.9%)	0.0024 (7.2%)
$\Delta\Gamma$	0.0047 (0.6%)	—
Fraction of wrong PV component	0.0021 (0.3%)	0.0011 (3.3%)
z -scale	0.0012 (0.2%)	0.0023 (7.0%)
Δm	—	0.0034 (10.3%)
Upper decay time acceptance	—	0.0012 (3.6%)
Correlation between mass and decay time	—	—
Decay time resolution calibration	—	—
Decay time resolution offset	—	—
Low decay time acceptance	—	—
Production asymmetry	—	—
Sum	0.020 (2.7%)	0.005 (15.2%)

LHCb collaboration

R. Aaij⁴¹, B. Adeva³⁷, M. Adinolfi⁴⁶, A. Affolder⁵², Z. Ajaltouni⁵, S. Akar⁶, J. Albrecht⁹, F. Alessio³⁸, M. Alexander⁵¹, S. Ali⁴¹, G. Alkhazov³⁰, P. Alvarez Cartelle⁵³, A.A. Alves Jr⁵⁷, S. Amato², S. Amerio²², Y. Amhis⁷, L. An³, L. Anderlini^{17,g}, J. Anderson⁴⁰, M. Andreotti^{16,f}, J.E. Andrews⁵⁸, R.B. Appleby⁵⁴, O. Aquines Gutierrez¹⁰, F. Archilli³⁸, A. Artamonov³⁵, M. Artuso⁵⁹, E. Aslanides⁶, G. Auriemma^{25,n}, M. Baalouch⁵, S. Bachmann¹¹, J.J. Back⁴⁸, A. Badalov³⁶, C. Baesso⁶⁰, W. Baldini^{16,38}, R.J. Barlow⁵⁴, C. Barschel³⁸, S. Barsuk⁷, W. Barter³⁸, V. Batozskaya²⁸, V. Battista³⁹, A. Bay³⁹, L. Beaucourt⁴, J. Beddow⁵¹, F. Bedeschi²³, I. Bediaga¹, L.J. Bel⁴¹, I. Belyaev³¹, E. Ben-Haim⁸, G. Bencivenni¹⁸, S. Benson³⁸, J. Benton⁴⁶, A. Berezhnoy³², R. Bernet⁴⁰, A. Bertolin²², M.-O. Bettler³⁸, M. van Beuzekom⁴¹, A. Bien¹¹, S. Bifani⁴⁵, T. Bird⁵⁴, A. Birnkraut⁹, A. Bizzeti^{17,i}, T. Blake⁴⁸, F. Blanc³⁹, J. Blouw¹⁰, S. Blusk⁵⁹, V. Bocci²⁵, A. Bondar³⁴, N. Bondar^{30,38}, W. Bonivento¹⁵, S. Borghi⁵⁴, A. Borgia⁵⁹, M. Borsato⁷, T.J.V. Bowcock⁵², E. Bowen⁴⁰, C. Bozzi¹⁶, S. Braun¹¹, D. Brett⁵⁴, M. Britsch¹⁰, T. Britton⁵⁹, J. Brodzicka⁵⁴, N.H. Brook⁴⁶, A. Bursche⁴⁰, J. Buytaert³⁸, S. Cadeddu¹⁵, R. Calabrese^{16,f}, M. Calvi^{20,k}, M. Calvo Gomez^{36,p}, P. Campana¹⁸, D. Campora Perez³⁸, L. Capriotti⁵⁴, A. Carbone^{14,d}, G. Carboni^{24,l}, R. Cardinale^{19,j}, A. Cardini¹⁵, P. Carniti²⁰, L. Carson⁵⁰, K. Carvalho Akiba^{2,38}, R. Casanova Mohr³⁶, G. Casse⁵², L. Cassina^{20,k}, L. Castillo Garcia³⁸, M. Cattaneo³⁸, Ch. Cauet⁹, G. Cavallero¹⁹, R. Cenci^{23,t}, M. Charles⁸, Ph. Charpentier³⁸, M. Chefdeville⁴, S. Chen⁵⁴, S.-F. Cheung⁵⁵, N. Chiapolini⁴⁰, M. Chrzaszcz^{40,26}, X. Cid Vidal³⁸, G. Ciezarek⁴¹, P.E.L. Clarke⁵⁰, M. Clemencic³⁸, H.V. Cliff⁴⁷, J. Closier³⁸, V. Coco³⁸, J. Cogan⁶, E. Cogneras⁵, V. Cogoni^{15,e}, L. Cojocariu²⁹, G. Collazuol²², P. Collins³⁸, A. Comerma-Montells¹¹, A. Contu^{15,38}, A. Cook⁴⁶, M. Coombes⁴⁶, S. Coquereau⁸, G. Corti³⁸, M. Corvo^{16,f}, I. Counts⁵⁶, B. Couturier³⁸, G.A. Cowan⁵⁰, D.C. Craik⁴⁸, A.C. Crocombe⁴⁸, M. Cruz Torres⁶⁰, S. Cunliffe⁵³, R. Currie⁵³, C. D'Ambrosio³⁸, J. Dalseno⁴⁶, P.N.Y. David⁴¹, A. Davis⁵⁷, K. De Bruyn⁴¹, S. De Capua⁵⁴, M. De Cian¹¹, J.M. De Miranda¹, L. De Paula², W. De Silva⁵⁷, P. De Simone¹⁸, C.-T. Dean⁵¹, D. Decamp⁴, M. Deckenhoff⁹, L. Del Buono⁸, N. Déléage⁴, D. Derkach⁵⁵, O. Deschamps⁵, F. Dettori³⁸, B. Dey⁴⁰, A. Di Canto³⁸, F. Di Ruscio²⁴, H. Dijkstra³⁸, S. Donleavy⁵², F. Dordei¹¹, M. Dorigo³⁹, A. Dosil Suárez³⁷, D. Dossett⁴⁸, A. Dovbnya⁴³, K. Dreimanis⁵², G. Dujany⁵⁴, F. Dupertuis³⁹, P. Durante³⁸, R. Dzhelyadin³⁵, A. Dziurda²⁶, A. Dzyuba³⁰, S. Easo^{49,38}, U. Egede⁵³, V. Egorychev³¹, S. Eidelman³⁴, S. Eisenhardt⁵⁰, U. Eitschberger⁹, R. Ekelhof⁹, L. Eklund⁵¹, I. El Rifai⁵, Ch. Elsasser⁴⁰, S. Ely⁵⁹, S. Esen¹¹, H.M. Evans⁴⁷, T. Evans⁵⁵, A. Falabella¹⁴, C. Färber¹¹, C. Farinelli⁴¹, N. Farley⁴⁵, S. Farry⁵², R. Fay⁵², D. Ferguson⁵⁰, V. Fernandez Albor³⁷, F. Ferrari¹⁴, F. Ferreira Rodrigues¹, M. Ferro-Luzzi³⁸, S. Filippov³³, M. Fiore^{16,38,f}, M. Fiorini^{16,f}, M. Firlej²⁷, C. Fitzpatrick³⁹, T. Fiutowski²⁷, P. Fol⁵³, M. Fontana¹⁰, F. Fontanelli^{19,j}, R. Forty³⁸, O. Francisco², M. Frank³⁸, C. Frei³⁸, M. Frosini¹⁷, J. Fu^{21,38}, E. Furfarò^{24,l}, A. Gallas Torreira³⁷, D. Galli^{14,d}, S. Gallorini^{22,38}, S. Gambetta^{19,j}, M. Gandelman², P. Gandini⁵⁵, Y. Gao³, J. García Pardiñas³⁷, J. Garofoli⁵⁹, J. Garra Tico⁴⁷, L. Garrido³⁶, D. Gascon³⁶, C. Gaspar³⁸, U. Gastaldi¹⁶, R. Gauld⁵⁵, L. Gavardi⁹, G. Gazzoni⁵, A. Geraci^{21,v}, D. Gerick¹¹, E. Gersabeck¹¹, M. Gersabeck⁵⁴, T. Gershon⁴⁸, Ph. Ghez⁴, A. Gianelle²², S. Giani³⁹, V. Gibson⁴⁷, L. Giubega²⁹, V.V. Gligorov³⁸, C. Göbel⁶⁰, D. Golubkov³¹, A. Golutvin^{53,31,38}, A. Gomes^{1,a}, C. Gotti^{20,k}, M. Grabalosa Gándara⁵, R. Graciani Diaz³⁶, L.A. Granado Cardoso³⁸, E. Graugés³⁶, E. Graverini⁴⁰, G. Graziani¹⁷, A. Grecu²⁹, E. Greening⁵⁵, S. Gregson⁴⁷, P. Griffith⁴⁵, L. Grillo¹¹, O. Grünberg⁶³, E. Gushchin³³, Yu. Guz^{35,38}, T. Gys³⁸, C. Hadjivasiliou⁵⁹, G. Haefeli³⁹, C. Haen³⁸,

S.C. Haines⁴⁷, S. Hall⁵³, B. Hamilton⁵⁸, T. Hampson⁴⁶, X. Han¹¹, S. Hansmann-Menzemer¹¹, N. Harnew⁵⁵, S.T. Harnew⁴⁶, J. Harrison⁵⁴, J. He³⁸, T. Head³⁹, V. Heijne⁴¹, K. Hennessy⁵², P. Henrard⁵, L. Henry⁸, J.A. Hernando Morata³⁷, E. van Herwijnen³⁸, M. Hef⁶³, A. Hicheur², D. Hill⁵⁵, M. Hoballah⁵, C. Hombach⁵⁴, W. Hulsbergen⁴¹, T. Humair⁵³, N. Hussain⁵⁵, D. Hutchcroft⁵², D. Hynds⁵¹, M. Idzik²⁷, P. Ilten⁵⁶, R. Jacobsson³⁸, A. Jaeger¹¹, J. Jalocha⁵⁵, E. Jans⁴¹, A. Jawahery⁵⁸, F. Jing³, M. John⁵⁵, D. Johnson³⁸, C.R. Jones⁴⁷, C. Joram³⁸, B. Jost³⁸, N. Jurik⁵⁹, S. Kandybei⁴³, W. Kanso⁶, M. Karacson³⁸, T.M. Karbach³⁸, S. Karodia⁵¹, M. Kelsey⁵⁹, I.R. Kenyon⁴⁵, M. Kenzie³⁸, T. Ketel⁴², B. Khanji^{20,38,k}, C. Khurewathanakul³⁹, S. Klaver⁵⁴, K. Klimaszewski²⁸, O. Kochebina⁷, M. Kolpin¹¹, I. Komarov³⁹, R.F. Koopman⁴², P. Koppenburg^{41,38}, M. Korolev³², L. Kravchuk³³, K. Kreplin¹¹, M. Kreps⁴⁸, G. Krocker¹¹, P. Krokovny³⁴, F. Kruse⁹, W. Kucewicz^{26,o}, M. Kucharczyk²⁶, V. Kudryavtsev³⁴, K. Kurek²⁸, T. Kvaratskheliya³¹, V.N. La Thi³⁹, D. Lacarrere³⁸, G. Lafferty⁵⁴, A. Lai¹⁵, D. Lambert⁵⁰, R.W. Lambert⁴², G. Lanfranchi¹⁸, C. Langenbruch⁴⁸, B. Langhans³⁸, T. Latham⁴⁸, C. Lazzeroni⁴⁵, R. Le Gac⁶, J. van Leerdam⁴¹, J.-P. Lees⁴, R. Lefevre⁵, A. Leflat³², J. Lefrançois⁷, O. Leroy⁶, T. Lesiak²⁶, B. Leverington¹¹, Y. Li⁷, T. Likhomanenko⁶⁴, M. Liles⁵², R. Lindner³⁸, C. Linn³⁸, F. Lionetto⁴⁰, B. Liu¹⁵, S. Lohn³⁸, I. Longstaff⁵¹, J.H. Lopes², P. Lowdon⁴⁰, D. Lucchesi^{22,r}, H. Luo⁵⁰, A. Lupato²², E. Luppi^{16,f}, O. Lupton⁵⁵, F. Machefert⁷, I.V. Machikhiliyan³¹, F. Maciuc²⁹, O. Maev³⁰, S. Malde⁵⁵, A. Malinin⁶⁴, G. Manca^{15,e}, G. Mancinelli⁶, P. Manning⁵⁹, A. Mapelli³⁸, J. Maratas⁵, J.F. Marchand⁴, U. Marconi¹⁴, C. Marin Benito³⁶, P. Marino^{23,38,t}, R. Märki³⁹, J. Marks¹¹, G. Martellotti²⁵, M. Martinelli³⁹, D. Martinez Santos⁴², F. Martinez Vidal⁶⁶, D. Martins Tostes², A. Massafferri¹, R. Matev³⁸, Z. Mathe³⁸, C. Matteuzzi²⁰, A. Mauri⁴⁰, B. Maurin³⁹, A. Mazurov⁴⁵, M. McCann⁵³, J. McCarthy⁴⁵, A. McNab⁵⁴, R. McNulty¹², B. McSkelly⁵², B. Meadows⁵⁷, F. Meier⁹, M. Meissner¹¹, M. Merk⁴¹, D.A. Milanes⁶², M.-N. Minard⁴, D.S. Mitzel¹¹, J. Molina Rodriguez⁶⁰, S. Monteil⁵, M. Morandin²², P. Morawski²⁷, A. Mordà⁶, M.J. Morello^{23,t}, J. Moron²⁷, A.-B. Morris⁵⁰, R. Mountain⁵⁹, F. Muheim⁵⁰, K. Müller⁴⁰, V. Müller⁹, M. Mussini¹⁴, B. Muster³⁹, P. Naik⁴⁶, T. Nakada³⁹, R. Nandakumar⁴⁹, I. Nasteva², M. Needham⁵⁰, N. Neri²¹, S. Neubert¹¹, N. Neufeld³⁸, M. Neuner¹¹, A.D. Nguyen³⁹, T.D. Nguyen³⁹, C. Nguyen-Mau^{39,q}, V. Niess⁵, R. Niet⁹, N. Nikitin³², T. Nikodem¹¹, A. Novoselov³⁵, D.P. O'Hanlon⁴⁸, A. Oblakowska-Mucha²⁷, V. Obraztsov³⁵, S. Ogilvy⁵¹, O. Okhrimenko⁴⁴, R. Oldeman^{15,e}, C.J.G. Onderwater⁶⁷, B. Osorio Rodrigues¹, J.M. Otalora Goicochea², A. Otto³⁸, P. Owen⁵³, A. Oyanguren⁶⁶, A. Palano^{13,c}, F. Palombo^{21,u}, M. Palutan¹⁸, J. Panman³⁸, A. Papanestis⁴⁹, M. Pappagallo⁵¹, L.L. Pappalardo^{16,f}, C. Parkes⁵⁴, G. Passaleva¹⁷, G.D. Patel⁵², M. Patel⁵³, C. Patrignani^{19,j}, A. Pearce^{54,49}, A. Pellegrino⁴¹, G. Penso^{25,m}, M. Pepe Altarelli³⁸, S. Perazzini^{14,d}, P. Perret⁵, L. Pescatore⁴⁵, K. Petridis⁴⁶, A. Petrolini^{19,j}, E. Picatoste Olloqui³⁶, B. Pietrzyk⁴, T. Pilar⁴⁸, D. Pinci²⁵, A. Pistone¹⁹, S. Playfer⁵⁰, M. Plo Casasus³⁷, T. Poikela³⁸, F. Polci⁸, A. Poluektov^{48,34}, I. Polyakov³¹, E. Polycarpo², A. Popov³⁵, D. Popov¹⁰, B. Popovici²⁹, C. Potterat², E. Price⁴⁶, J.D. Price⁵², J. Prisciandaro³⁹, A. Pritchard⁵², C. Prouve⁴⁶, V. Pugatch⁴⁴, A. Puig Navarro³⁹, G. Punzi^{23,s}, W. Qian⁴, R. Quagliani^{7,46}, B. Rachwal²⁶, J.H. Rademacker⁴⁶, B. Rakotomiaramanana³⁹, M. Rama²³, M.S. Rangel², I. Raniuk⁴³, N. Rauschmayr³⁸, G. Raven⁴², F. Redi⁵³, S. Reichert⁵⁴, M.M. Reid⁴⁸, A.C. dos Reis¹, S. Ricciardi⁴⁹, S. Richards⁴⁶, M. Rihl³⁸, K. Rinnert⁵², V. Rives Molina³⁶, P. Robbe^{7,38}, A.B. Rodrigues¹, E. Rodrigues⁵⁴, J.A. Rodriguez Lopez⁶², P. Rodriguez Perez⁵⁴, S. Roiser³⁸, V. Romanovsky³⁵, A. Romero Vidal³⁷, M. Rotondo²², J. Rouvinet³⁹, T. Ruf³⁸, H. Ruiz³⁶, P. Ruiz Valls⁶⁶, J.J. Saborido Silva³⁷, N. Sagidova³⁰, P. Sail⁵¹, B. Saitta^{15,e}, V. Salustino Guimaraes², C. Sanchez Mayordomo⁶⁶, B. Sanmartin Sedes³⁷, R. Santacesaria²⁵,

C. Santamarina Rios³⁷, E. Santovetti^{24,l}, A. Sarti^{18,m}, C. Satriano^{25,n}, A. Satta²⁴, D.M. Saunders⁴⁶, D. Savrina^{31,32}, M. Schellenberg⁹, M. Schiller³⁸, H. Schindler³⁸, M. Schlupp⁹, M. Schmelling¹⁰, B. Schmidt³⁸, O. Schneider³⁹, A. Schopper³⁸, M.-H. Schune⁷, R. Schwemmer³⁸, B. Sciascia¹⁸, A. Sciubba^{25,m}, A. Semennikov³¹, I. Sepp⁵³, N. Serra⁴⁰, J. Serrano⁶, L. Sestini²², P. Seyfert¹¹, M. Shapkin³⁵, I. Shapoval^{16,43,f}, Y. Shcheglov³⁰, T. Shears⁵², L. Shekhtman³⁴, V. Shevchenko⁶⁴, A. Shires⁹, R. Silva Coutinho⁴⁸, G. Simi²², M. Sirendi⁴⁷, N. Skidmore⁴⁶, I. Skillicorn⁵¹, T. Skwarnicki⁵⁹, N.A. Smith⁵², E. Smith^{55,49}, E. Smith⁵³, J. Smith⁴⁷, M. Smith⁵⁴, H. Snoek⁴¹, M.D. Sokoloff^{57,38}, F.J.P. Soler⁵¹, F. Soomro³⁹, D. Souza⁴⁶, B. Souza De Paula², B. Spaan⁹, P. Spradlin⁵¹, S. Sridharan³⁸, F. Stagni³⁸, M. Stahl¹¹, S. Stahl³⁸, O. Steinkamp⁴⁰, O. Stenyakin³⁵, F. Sterpka⁵⁹, S. Stevenson⁵⁵, S. Stoica²⁹, S. Stone⁵⁹, B. Storaci⁴⁰, S. Stracka^{23,t}, M. Straticiuc²⁹, U. Straumann⁴⁰, R. Stroili²², L. Sun⁵⁷, W. Sutcliffe⁵³, K. Swientek²⁷, S. Swientek⁹, V. Syropoulos⁴², M. Szczekowski²⁸, P. Szczypka^{39,38}, T. Szumlak²⁷, S. T'Jampens⁴, M. Teklishyn⁷, G. Tellarini^{16,f}, F. Teubert³⁸, C. Thomas⁵⁵, E. Thomas³⁸, J. van Tilburg⁴¹, V. Tisserand⁴, M. Tobin³⁹, J. Todd⁵⁷, S. Tolk⁴², L. Tomassetti^{16,f}, D. Tonelli³⁸, S. Topp-Joergensen⁵⁵, N. Torr⁵⁵, E. Tournefier⁴, S. Tourneur³⁹, K. Trabelsi³⁹, M.T. Tran³⁹, M. Tresch⁴⁰, A. Trisovic³⁸, A. Tsaregorodtsev⁶, P. Tsopelas⁴¹, N. Tuning^{41,38}, M. Ubeda Garcia³⁸, A. Ukleja²⁸, A. Ustyuzhanin⁶⁵, U. Uwer¹¹, C. Vacca^{15,e}, V. Vagnoni¹⁴, G. Valenti¹⁴, A. Vallier⁷, R. Vazquez Gomez¹⁸, P. Vazquez Regueiro³⁷, C. Vázquez Sierra³⁷, S. Vecchi¹⁶, J.J. Velthuis⁴⁶, M. Veltri^{17,h}, G. Veneziano³⁹, M. Vesterinen¹¹, J.V. Viana Barbosa³⁸, B. Viaud⁷, D. Vieira², M. Vieites Diaz³⁷, X. Vilasis-Cardona^{36,p}, A. Vollhardt⁴⁰, D. Volyanskyy¹⁰, D. Voong⁴⁶, A. Vorobyev³⁰, V. Vorobyev³⁴, C. Voß⁶³, J.A. de Vries⁴¹, R. Waldi⁶³, C. Wallace⁴⁸, R. Wallace¹², J. Walsh²³, S. Wandernoth¹¹, J. Wang⁵⁹, D.R. Ward⁴⁷, N.K. Watson⁴⁵, D. Websdale⁵³, A. Weiden⁴⁰, M. Whitehead⁴⁸, D. Wiedner¹¹, G. Wilkinson^{55,38}, M. Wilkinson⁵⁹, M. Williams³⁸, M.P. Williams⁴⁵, M. Williams⁵⁶, F.F. Wilson⁴⁹, J. Wimberley⁵⁸, J. Wishahi⁹, W. Wislicki²⁸, M. Witek²⁶, G. Wormser⁷, S.A. Wotton⁴⁷, S. Wright⁴⁷, K. Wyllie³⁸, Y. Xie⁶¹, Z. Xu³⁹, Z. Yang³, X. Yuan³⁴, O. Yushchenko³⁵, M. Zangoli¹⁴, M. Zavertyaev^{10,b}, L. Zhang³, Y. Zhang³, A. Zhelezov¹¹, A. Zhokhov³¹, L. Zhong³.

¹Centro Brasileiro de Pesquisas Físicas (CBPF), Rio de Janeiro, Brazil

²Universidade Federal do Rio de Janeiro (UFRJ), Rio de Janeiro, Brazil

³Center for High Energy Physics, Tsinghua University, Beijing, China

⁴LAPP, Université Savoie Mont-Blanc, CNRS/IN2P3, Annecy-Le-Vieux, France

⁵Clermont Université, Université Blaise Pascal, CNRS/IN2P3, LPC, Clermont-Ferrand, France

⁶CPPM, Aix-Marseille Université, CNRS/IN2P3, Marseille, France

⁷LAL, Université Paris-Sud, CNRS/IN2P3, Orsay, France

⁸LPNHE, Université Pierre et Marie Curie, Université Paris Diderot, CNRS/IN2P3, Paris, France

⁹Fakultät Physik, Technische Universität Dortmund, Dortmund, Germany

¹⁰Max-Planck-Institut für Kernphysik (MPIK), Heidelberg, Germany

¹¹Physikalisches Institut, Ruprecht-Karls-Universität Heidelberg, Heidelberg, Germany

¹²School of Physics, University College Dublin, Dublin, Ireland

¹³Sezione INFN di Bari, Bari, Italy

¹⁴Sezione INFN di Bologna, Bologna, Italy

¹⁵Sezione INFN di Cagliari, Cagliari, Italy

¹⁶Sezione INFN di Ferrara, Ferrara, Italy

¹⁷Sezione INFN di Firenze, Firenze, Italy

¹⁸Laboratori Nazionali dell'INFN di Frascati, Frascati, Italy

¹⁹Sezione INFN di Genova, Genova, Italy

- ²⁰Sezione INFN di Milano Bicocca, Milano, Italy
²¹Sezione INFN di Milano, Milano, Italy
²²Sezione INFN di Padova, Padova, Italy
²³Sezione INFN di Pisa, Pisa, Italy
²⁴Sezione INFN di Roma Tor Vergata, Roma, Italy
²⁵Sezione INFN di Roma La Sapienza, Roma, Italy
²⁶Henryk Niewodniczanski Institute of Nuclear Physics Polish Academy of Sciences, Kraków, Poland
²⁷AGH - University of Science and Technology, Faculty of Physics and Applied Computer Science, Kraków, Poland
²⁸National Center for Nuclear Research (NCBJ), Warsaw, Poland
²⁹Horia Hulubei National Institute of Physics and Nuclear Engineering, Bucharest-Magurele, Romania
³⁰Petersburg Nuclear Physics Institute (PNPI), Gatchina, Russia
³¹Institute of Theoretical and Experimental Physics (ITEP), Moscow, Russia
³²Institute of Nuclear Physics, Moscow State University (SINP MSU), Moscow, Russia
³³Institute for Nuclear Research of the Russian Academy of Sciences (INR RAN), Moscow, Russia
³⁴Budker Institute of Nuclear Physics (SB RAS) and Novosibirsk State University, Novosibirsk, Russia
³⁵Institute for High Energy Physics (IHEP), Protvino, Russia
³⁶Universitat de Barcelona, Barcelona, Spain
³⁷Universidad de Santiago de Compostela, Santiago de Compostela, Spain
³⁸European Organization for Nuclear Research (CERN), Geneva, Switzerland
³⁹Ecole Polytechnique Fédérale de Lausanne (EPFL), Lausanne, Switzerland
⁴⁰Physik-Institut, Universität Zürich, Zürich, Switzerland
⁴¹Nikhef National Institute for Subatomic Physics, Amsterdam, The Netherlands
⁴²Nikhef National Institute for Subatomic Physics and VU University Amsterdam, Amsterdam, The Netherlands
⁴³NSC Kharkiv Institute of Physics and Technology (NSC KIPT), Kharkiv, Ukraine
⁴⁴Institute for Nuclear Research of the National Academy of Sciences (KINR), Kyiv, Ukraine
⁴⁵University of Birmingham, Birmingham, United Kingdom
⁴⁶H.H. Wills Physics Laboratory, University of Bristol, Bristol, United Kingdom
⁴⁷Cavendish Laboratory, University of Cambridge, Cambridge, United Kingdom
⁴⁸Department of Physics, University of Warwick, Coventry, United Kingdom
⁴⁹STFC Rutherford Appleton Laboratory, Didcot, United Kingdom
⁵⁰School of Physics and Astronomy, University of Edinburgh, Edinburgh, United Kingdom
⁵¹School of Physics and Astronomy, University of Glasgow, Glasgow, United Kingdom
⁵²Oliver Lodge Laboratory, University of Liverpool, Liverpool, United Kingdom
⁵³Imperial College London, London, United Kingdom
⁵⁴School of Physics and Astronomy, University of Manchester, Manchester, United Kingdom
⁵⁵Department of Physics, University of Oxford, Oxford, United Kingdom
⁵⁶Massachusetts Institute of Technology, Cambridge, MA, United States
⁵⁷University of Cincinnati, Cincinnati, OH, United States
⁵⁸University of Maryland, College Park, MD, United States
⁵⁹Syracuse University, Syracuse, NY, United States
⁶⁰Pontifícia Universidade Católica do Rio de Janeiro (PUC-Rio), Rio de Janeiro, Brazil, associated to ²
⁶¹Institute of Particle Physics, Central China Normal University, Wuhan, Hubei, China, associated to ³
⁶²Departamento de Física , Universidad Nacional de Colombia, Bogota, Colombia, associated to ⁸
⁶³Institut für Physik, Universität Rostock, Rostock, Germany, associated to ¹¹
⁶⁴National Research Centre Kurchatov Institute, Moscow, Russia, associated to ³¹
⁶⁵Yandex School of Data Analysis, Moscow, Russia, associated to ³¹
⁶⁶Instituto de Física Corpuscular (IFIC), Universitat de Valencia-CSIC, Valencia, Spain, associated to ³⁶
⁶⁷Van Swinderen Institute, University of Groningen, Groningen, The Netherlands, associated to ⁴¹

^aUniversidade Federal do Triângulo Mineiro (UFTM), Uberaba-MG, Brazil

- ^b*P.N. Lebedev Physical Institute, Russian Academy of Science (LPI RAS), Moscow, Russia*
- ^c*Università di Bari, Bari, Italy*
- ^d*Università di Bologna, Bologna, Italy*
- ^e*Università di Cagliari, Cagliari, Italy*
- ^f*Università di Ferrara, Ferrara, Italy*
- ^g*Università di Firenze, Firenze, Italy*
- ^h*Università di Urbino, Urbino, Italy*
- ⁱ*Università di Modena e Reggio Emilia, Modena, Italy*
- ^j*Università di Genova, Genova, Italy*
- ^k*Università di Milano Bicocca, Milano, Italy*
- ^l*Università di Roma Tor Vergata, Roma, Italy*
- ^m*Università di Roma La Sapienza, Roma, Italy*
- ⁿ*Università della Basilicata, Potenza, Italy*
- ^o*AGH - University of Science and Technology, Faculty of Computer Science, Electronics and Telecommunications, Kraków, Poland*
- ^p*LIFAELS, La Salle, Universitat Ramon Llull, Barcelona, Spain*
- ^q*Hanoi University of Science, Hanoi, Viet Nam*
- ^r*Università di Padova, Padova, Italy*
- ^s*Università di Pisa, Pisa, Italy*
- ^t*Scuola Normale Superiore, Pisa, Italy*
- ^u*Università degli Studi di Milano, Milano, Italy*
- ^v*Politecnico di Milano, Milano, Italy*